Restoration of Retinal Images Obtained Through Cataracts

ELI PELI, MEMBER, IEEE, AND TAMAR PELI, MEMBER, IEEE

Abstract—**An optical model for imaging the retina through cataract has been developed. The images are treated as sample functions of stochastic processes. Based on this model, a homomorphic Wiener filter can be designed that will optimally restore the cataractous image (in the mean-square error sense). The design of the filter requires *a priori* knowledge of the statistics of either the cataract transmittance function or the noncataractous image. The cataract transmittance function, assumed to be low pass in nature, can be estimated from the cataractous image of the retina. The statistics of the noncataractous image may be estimated using an old, precataractous photograph of the same retina, which is frequently available. Various modes of this restoration concept were applied to clinical photographs and found to be effective. The best results were obtained with short-space enhancement using averaged short-space estimates of the spectra of the two images.**

I. Introduction

RETINAL images are routinely used in ophthalmic practice for diagnosis and follow-up of eye diseases. Retinal photographs are of great value to physicians for detecting subtle fundus changes that may occur over time. As many eye diseases are associated with old age, the quality of the retinal image is frequently reduced by light scatter from cataracts and other ocular media turbidity. The degradation of image quality by cataract may greatly impede visual inspection and automated image processing of the photographs.

Various techniques to improve fundus visibility in the presence of media turbidity were investigated. Most commonly, the optical system has been modified in an effort to separate the illumination and imaging pathways at the patient's pupil to reduce specular reflections and backscatter from the cataract [1]–[3]. Modification of the photographic technique [4] and the use of various filters [5] may be helpful. However, even with the best techniques, the cataract may degrade the image significantly.

In the presence of moderate turbidity, the general appearance of the retina is clear, but very fine details such as the retinal nerve fiber layer or small arteries in fluorescein angiography are difficult to evaluate. With the increased application of digital image processing to retinal imaging in recent years [6], image-enhancement techniques have been used to improve the visibility of fundus details [6], [7] from photographs taken through relatively clear media. Peli and Schwartz [8] have shown that enhancement of fundus photographs taken through cataracts is feasible and clinically valuable. This paper presents an improved model for the imaging process, which results in optimal restoration (in the mean-square error sense).

Manuscript received November 21, 1988; revised May 31, 1989. This work was supported in part by Grants EY05450 and EY05957 from the National Institutes of Health and a grant from the Alcoa Foundation.

E. Peli is with the Eye Research Institute of Retina Foundation, Boston, MA 02114, the Department of Ophthalmology, Harvard Medical School, Boston, MA 02115, and the Department of Ophthalmology, Tufts University School of Medicine, Boston, MA 02111.

T. Peli is with Atlantic Aerospace Electronics Corporation, Waltham, MA 02154.

IEEE Log Number 8929786.

II. Imaging Model and Filtering

The model for imaging the retina in photographs taken through cataract is similar to the model used to represent imaging of the earth from a satellite in the presence of light cloud cover [9], [10]. In this model (Fig. 1), the recorded image is composed of retinal reflectance information and light reflected back from the cataract:

$$s(x, y) = a \cdot L \cdot r(x, y) \cdot t(x, y) + L[1 - t(x, y)] \tag{1}$$

where $0 \leq r(x, y) \leq 1$ is the retinal reflectance function and $0 \leq t(x, y) \leq 1$ is the transmittance function of the cataract representing the noise in the system. The only coordinates system used is referred to the film plane where all the relevant imaging takes place. Thus, $r(x, y)$ includes all the distortions associated with the optics of the eye and the fundus camera, as well as the effect of the slight curvature of the retinal plane. Since the crystalline lens is not in focus at the film plane, the effects of $t(x, y)$ at that plane will be low pass in character, even if high-frequency details exist in the lens itself. L is the flash illumination of the fundus camera and a is the attenuation of retinal illumination due to the cataract. The illumination beam is condensed to intersect only a thin ring at the periphery of the eye's lens [1], and therefore, a constant can be used in this case. In addition, the cataract is highly out of focus on the retina, and even a sharp opacity on the lens will result only in a uniform reduction of the retinal illumination and will not cast a local shadow. Absorption reduces the light reaching the retina only in nuclear sclerotic cataracts [11]. Those cataracts are less common in patients younger than 70 years old [11], and even when they exist, they account for a small and fairly uniform light loss.

Peli and Schwartz [8] used simpler models, both of which are submodels of (1). For homomorphic filtering

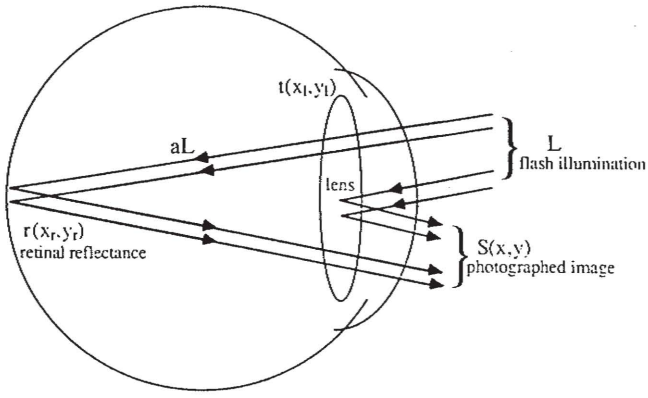

Fig. 1. A model for imaging the retina through a cataractous lens. The formed image is degraded by the cataract transmittance function multiplicatively, as well as additively, via the effect of the light backscattered from the lens. Both coordinate systems attached to the retinal (x_r, y_r) and lenticular $(x_l y_l)$ planes are referred to the film plane coordinates in (1).

[12], it was assumed that the recorded image was

$$s(x, y) = r(x, y) \cdot t(x, y) \tag{2}$$

representing only the first part of (1) and ignoring the effects of backscattered light. In the adaptive enhancement [13] technique, the image was assumed to be constructed according to

$$s(x, y) = r(x, y) + L[1 - t(x, y)], \tag{3}$$

i.e., ignoring the multiplicative effect of the cataract degradation on the image.

Equation (1) can be rearranged and written in the form

$$L - s(x, y) = t(x, y) \cdot [L - a \cdot L \cdot r(x, y)]. \tag{4}$$

This is a multiplicative expression for the noise and the image. By taking the logarithm of (4), one obtains an additive expression of signal and noise [12]:

$$\log [L - s(x, y)] = \log [L - a \cdot L \cdot r(x, y)] + \log [t(x, y)]. \tag{5}$$

This can be expressed as

$$P(x, y) = M(x, y) + N(x, y) \tag{6}$$

where $P(x, y)$, $M(x, y)$, and $N(x, y)$ are viewed as sample functions of stochastic processes, and

$$P(x, y) = \log [L - s(x, y)] = \text{signal} + \text{noise}$$

$$N(x, y) = \log [t(x, y)] = \text{noise}$$

$$M(x, y) = \log [L - a \cdot L \cdot r(x, y)] = \text{signal}.$$

$P(u, v)$, $M(u, v)$, and $N(u, v)$ are their respective Fourier transforms, with u and v the spatial frequency coordinates.

Linear filtering can be applied to estimate the signal when additive noise exists. If one assumes that signal and noise are not correlated (i.e., that the shape of the cataract has no correlation with the reflectance of the retina), the minimum mean-square error estimate of the signal can be obtained by filtering the degraded image with the optimal linear filter (Wiener filter) [14]:

$$H(u, v) = \frac{S_{MP}(u, v)}{S_{PP}(u, v)} \tag{7}$$

where $S_{PP}(u, v)$ is the power spectrum of the signal plus noise and $S_{MP}(u, v)$ is the cross-power spectrum of signal and signal plus noise.

When the filter is known, the restored image may be calculated as

$$\hat{M}(u, v) = P(u, v) \cdot H(u, v). \tag{8}$$

To calculate the filter, the cross-power spectrum $S_{MP}(u, v)$ is needed. The cross-correlation between signal and signal plus noise is given by

$$\begin{aligned} R_{MP}(\tau_x, \tau_y) &= E\{M(x + \tau_x, y + \tau_y) \\ &\quad \cdot [M(x, y) + N(x, y)]\} \\ &= R_{MM}(\tau_x, \tau_y) + \overline{M} \cdot \overline{N} \end{aligned} \tag{9}$$

where $\overline{M}$ and $\overline{N}$ are the means of the signal and the noise, respectively.

The corresponding power spectrum is thus

$$S_{MP}(u, v) = S_{MM}(u, v) + \overline{M} \cdot \overline{N}\delta(u, v) \tag{10}$$

where $\delta(u, v)$ is the two-dimensional Dirac delta function. $S_{MM}(u, v)$ cannot be directly estimated in most applications. In previous work [9], [10], $S_{MP}(u, v)$ was calculated based on an estimate of the noise $t(x, y)$.

For this purpose, $S_{MP}(u, v)$ can be calculated also as

$$S_{MP}(u, v) = S_{PP}(u, v) - S_{NN}(u, v) - \overline{M} \cdot \overline{N} \cdot \delta(u, v) \tag{11}$$

where $S_{NN}(u, v)$ is the power spectrum of the noise.

In many cases, there is little *a priori* information about the statistics of the noise or the nature of $t(x, y)$. In the case of clouds and cataracts, the only assumption used to estimate $t(x, y)$ is that it is low pass in nature.

In the case of fundus photographs, an old picture is often available of the same fundus $S_{\text{old}}(x, y)$ taken before the cataract developed. The older photograph can be used to estimate the power spectrum of $M(x, y)$, $S_{MM}(u, v)$, which is calculated from $\log [L - S_{\text{old}}(x, y)]$. Similarly, S_{PP} is then calculated from the cataractous image $P(x, y)$ and the filter is obtained as

$$H(u, v) = \frac{S_{MM}(u, v) + \overline{M} \cdot \overline{N}\delta(u, v)}{S_{PP}(u, v)} \tag{12}$$

where

$$\overline{N} = \overline{P} - \overline{M} = S_{PP}(0, 0) - S_{MM}(0, 0). \tag{13}$$

The Fourier transform of the restored image is calculated as in (8). It is transformed back to the space domain via the inverse FFT to obtain an estimate of $\log [(L - a \cdot L \cdot r(x, y)]$. The final image $a \cdot L \cdot r(x, y)$ is then derived by antilog and subtraction from L.

III. Methods of Restoration

The restoration of cataractous retinal images was achieved through four different methods. In the first, no

precataractous image is available, and thus the noise has to be estimated from the cataractous image only. The other three methods use two ways of estimating the spectrum from a sample image (either by use of subsegments [for methods C and D] or the use of the whole image at once [method B]), and two ways of applying the filter to the image (again, segment by segment [method D] or to the whole image globally [methods B and C]).

A. Noise Estimation

If prior knowledge of the statistics of the retinal image (i.e., its spectrum) is not available, the filter can be calculated from the degraded image using the assumption that $t(x, y)$ is low pass in nature.

The cataract transmittance function $t(x, y)$ may be estimated from (1) as

$$t(x, y) = \frac{L - s(x, y)}{L - G} \tag{14}$$

where L is the estimate of the flash light and G is a constant representing the mean retinal reflectance. This function may then be low-pass filtered at an arbitrary level to obtain an estimate of the noise: $N(x, y) = \log [t(x, y)]$. An estimate of the spectrum of a signal may be calculated as the squared magnitude of the 2-D FFT (the periodogram). The spectrum of the noise $S_{NN}(u, v)$ is used for calculating the filter in (11). The filter was applied recursively, with the noise estimate updated at every step. The FFT of the whole image was used for spectrum estimation.

B. Full-Image Spectrum Estimation

The filter of (10) is calculated from the spectrum of the cataractous and precataractous images and applied to the FFT of the cataractous image. The simplest method for estimating the spectrum is to calculate the periodogram of the whole image at once. This is done for both the precataractous and the degraded images. The filter is calculated and applied to the FFT of the cataractous image.

C. Filter Expansion

The periodogram is a poor estimator of the spectrum [15]; a better estimate may be obtained by sectioning the image into smaller subimages that may partially overlap. The periodogram of each subimage was calculated, and the average of all periodograms served as an etimate of the spectra. This requires stationarity of the image as a stochastic process sample. The filter equation obtained in this manner was of subimage size and, therefore, could not be applied directly in the frequency domain to the full cataractous image. The filter was expanded to image size by interpolation. The interpolation was performed via FFT, by addition of zeros to expand the array to the image size, and then applying the inverse FFT to return to the filter domain with full image size. The *expanded filter* was applied to the FFT of the cataractous image as in the previous case.

D. Short Space Implementation

Another approach to the application of a subimage size filter to the larger image is called the *short space* implementation. The subimage size filter is first smoothed using a 3×3 square averaging window. The filter is then applied to overlapping sections of the same size to process the image one section at a time. The subimage sections are prewindowed with a two-dimensional triangular window. The window is matched to the overlapping area in such a way that simple addition of the overlapping segments point by point results in a weighted averaging of the enhanced segments. The final image is linearly scaled to the full dynamic range of the display. In the limit where the overlap is complete, this technique becomes very similar to the filter-expansion method.

IV. Experimental Materials

Retinal photographs were examined of six patients for whom, in addition to a cataractous image, a precataractous, clearer image was available. The color transparencies were digitized with a linear array CCD camera through a green filter, which enhances the contrast of the vasculature in the image. The digitized image pairs were processed by each of the four techniques of image restoration described in the previous section, and results were displayed on a monitor and photographed.

V. Results

The results of processing retinal images with the four methods are illustrated in Fig. 2. The clear precataract image taken in 1983 is shown in Fig. 2(a); the degraded image taken through the cataract in 1985 is shown in Fig. 2(b). The result of restoring the cataractous image using the noise estimation method, without use of the clear precataract image, is illustrated in Fig. 2(c). Fig. 2(d) represents an additional iteration of the same processing using the noise estimation method. The second iteration does not improve the image, and may even be considered inferior to the result of the first iteration. The filters used to obtain these images are presented in Fig. 2(e) and (f). As can be seen, the filter of the second iteration does little to change the image, indicating that all of the restoration that could have been achieved with this level of knowledge (i.e., low-pass filtering) is obtained in the first iteration.

Using the precataract clear image to estimate the spectrum of the image enables us to calculate the filter without any specific *a priori* notion of the spatial characteristics of the degradation process. The result of using this method, when the spectrum is estimated from the periodogram of the full image, is illustrated in Fig. 2(g). The filter used to obtain that image is illustrated in Fig. 2(h). This filter has essentially high-pass filtering characteristics, with some specific directional sensitivities. The processed image appears to be worse than the restoration with noise estimation for this case, although for some of the other cases, the quality of the image was better with this technique.

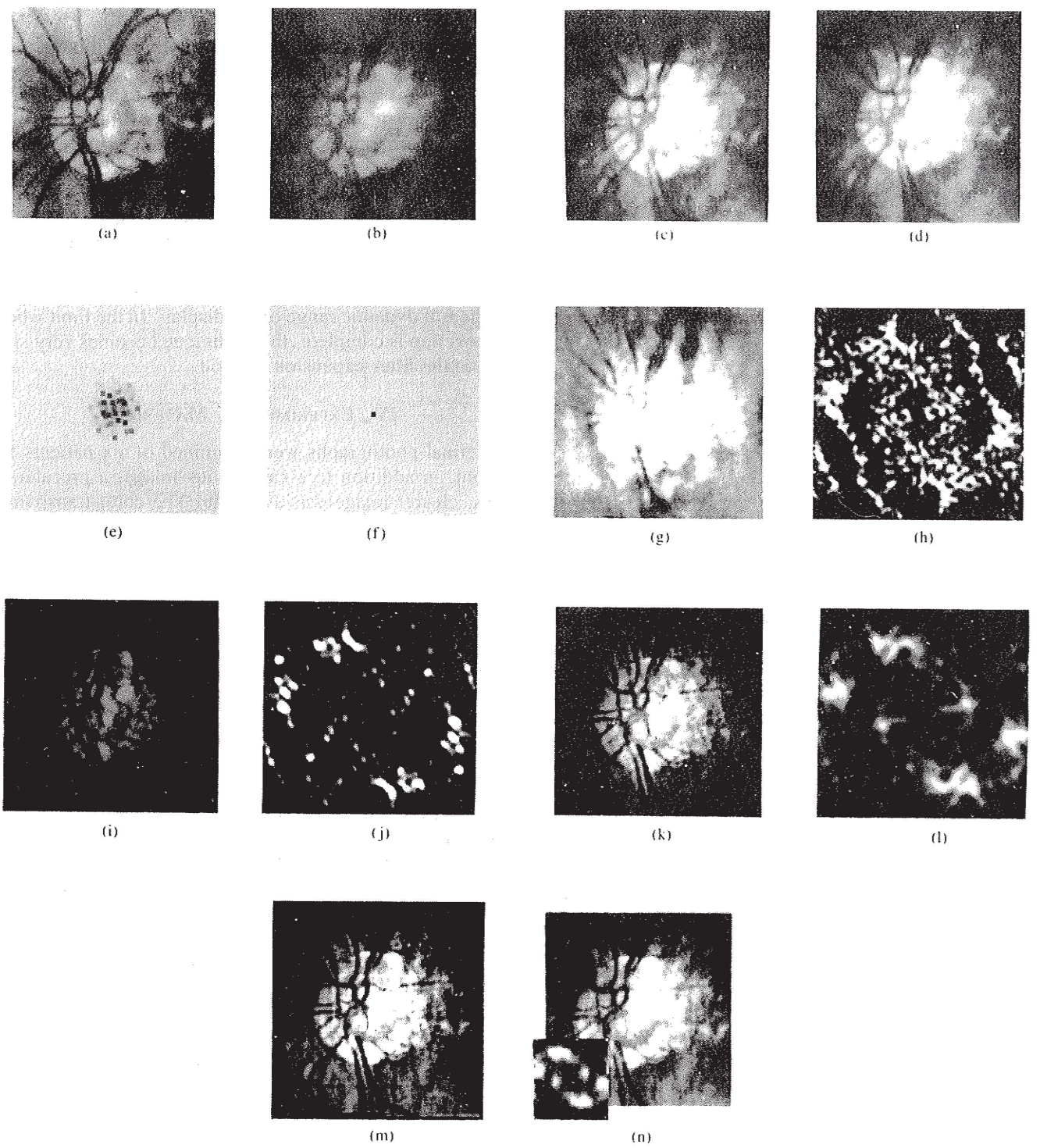

Fig. 2. Results of restoring the cataractous image with the various techniques: case 1. (a) Precataract image taken in 1983. (b) Cataractous image taken in 1985. (c) Restoration of the image in (b) using the noise estimation method. (d) Result of a second iteration of the method of noise estimation. The image in (c) was used as the degraded image in this case. (e) Filter used to obtain the image in (c) from the image in (b). The filter illustrated is in the spatial frequency domain with the dc at the center. The brightness at any point corresponds to the gain of the filter at that spatial frequency. (f) Filter used for the second iteration to obtain the image in (d) from the image in (c). (g) Result of restoring the image in (b) using the spectrum of the image in (a) with the full-image spectrum method. (h) Filter used to obtain the image in (g). (i) Result of restoring the image in (b) using 64 × 64 size windows to estimate the spectrum for the expanded filter applications. (j) Expanded filter used to obtain the image in (i). (k) Result of restoring the image in (b) using 32 × 32 windows for expanded filter. (l) Expanded filter used to obtain the image in (k). (m) Result of short space application of the 32 × 32 size filter shown in (k) to the image in (b) without expanding the filter and using 50 percent overlap. (n) Same technique as in (m) with 16 × 16 windows and filters. The bright edge represents an eight pixel wide edge effect of the triangular window which was compensated for in (m). The filter calculated and used is illustrated in the inset.

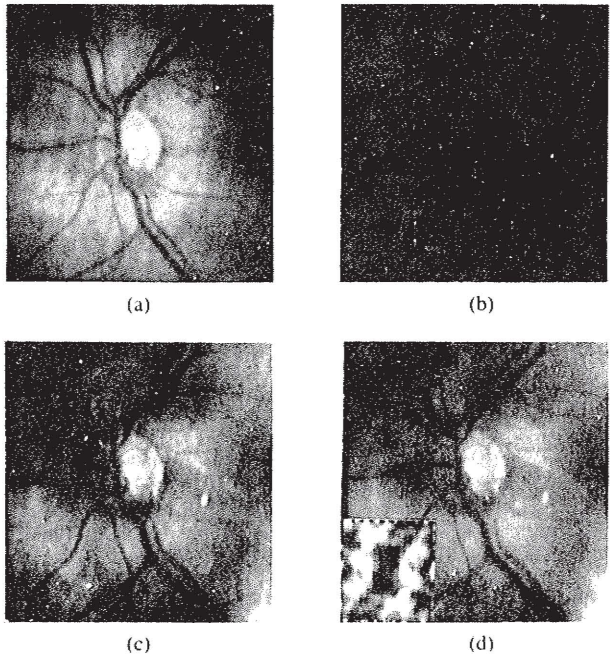

Fig. 3. Results of restoration: case 2. (a) Precataractous image. (b) Cataractous image. (c) Result of enhancing the image in (b) using the short space application of the 32 × 32 size filter with 50 percent overlap. (d) Result of enhancing the same image with 16 × 16 windows and filter. The filter calculated and used is illustrated in the inset.

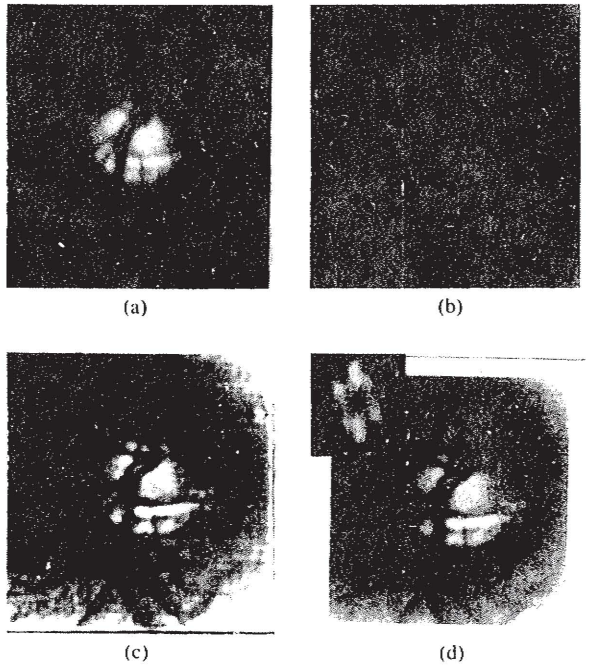

Fig. 4. Results of restoration: case 3. (a) Precataractous image. (b) Cataractous image. (c) Result of enhancing the image in (b) using the short space application of the 32 × 32 size filter with 50 percent overlap. (d) Result of enhancing the same image with 16 × 16 windows and filter. The filter calculated and used is illustrated in the inset.

A better estimate of the spectrum can be obtained by using sections of the image of size 64 × 64 with 50 percent overlap. The filter obtained should be expanded to the full 128 × 128 image size. The processed image is shown in Fig. 2(i), with the corresponding filter in Fig. 2(j). The expanded filter has the same general characteristics, with the scale remaining similar to the filter in Fig. 2(h). The processed image has slightly better quality for all cases tested. When smaller subsections of size 32 × 32 are used, the restoration is improved [Fig. 2(k)]. Again, the filter's shape and size [Fig. 2(l)] remain almost constant. These relationships actually illustrate the validity of the stationarity assumption.

Results of short space implementation are shown in Fig. 2(m) and (n), corresponding to a subimage size of 32 × 32 and 16 × 16, respectively. In both cases, an overlap of 50 percent was used to suppress block artifacts. These images represent the best restoration, and it appears that the filter size 32 × 32 resulted in better restoration than that achieved with the filter of size 16 × 16. Short space restoration is illustrated for two additional cases in Figs. 3 and 4.

VI. Discussion

Restoration of retinal images obtained through cataractous turbid media may be a valuable clinical tool [8]. Many of the visually disabling eye diseases such as glaucoma, age-related maculopathy, and diabetic retinopathy are associated with older age and frequently accompanied by turbidity or frank cataract of the crystalline lens. In the same way that image enhancement became an integral part of radiological imaging with the incorporation of computerized, digitized tomographic images, it may be expected that enhancement of retinal images will be used more frequently with the increased availability of electrooptical fundus imaging instruments, which provide digitized video images. Image processing capability is an integral part of many of these instruments; thus, basic tools for such enhancement will be available as well.

It is fortunate that in the case of retinal images, the spectrum of the undegraded image is frequently available. Even if an old, precataract, clear image of the same retina is not available, an image of the fellow eye may provide comparable spectral information. In cases where the other eye is also cataractous or not available for photography, images from eyes of other patients with similar racial and pigmentary characteristics can be used for an estimate of the spectrum. The same approach used here for retinal images may be used for any medical or other image-enhancement application where spectral estimation can be obtained from a previous or compatible image. Most retinal images are taken in one of two formats—centered either around the optic nerve head (as the images illustrated in this paper) or around the fovea, the center of high-resolution acuity. A "typical" spectrum for these two compositions may be obtained by averaging periodograms from many patients. Such averaged spectra may be used efficiently with the algorithms described here. A general spectral signature was previously used in the context of Weiner filtering [16], [17]. In most cases, only a one-dimensional, radially averaged spectrum of a "typical image" is used to represent spatial spectral characteristics [16], [18]. However, because in retinal images the

directions of the main vascular pattern are fairly consistent within images, a two-dimensional spectral estimate would result in better performance.

The proposed model offers a more complete modeling of the image degradation. This model is more appropriate for our case than it was for the removal of cloud cover where it was originally used [9]. Clouds do cast shadows on the earth rather than just decrease the illumination uniformly. In addition, the clouds, as well as the earth, are in focus for satellite imaging, while the cataract is out of focus, and thus, it is low-pass filtered in fundus photography. Most importantly, the availability of precataractous image enabled us to get a better estimate of image spectrum, the lack of which is often viewed as a great practical problem in applying the Wiener filter. With all these advantages, it was somewhat disappointing that the results were not much superior to results previously obtained with simpler models [8]. This is not surprising for the case of global processing because the spectrum estimation based on one image, without averaging, is not a good approximation. It was, therefore, expected that the expanded filter will result in better restoration, as it was based on a better estimate of the spectrum. The short space method resulted in the best restoration obtained so far, at the cost of increased computation. Short space processing has been shown to perform better [19] since it allows a more efficient use of the dynamic range of the image and it increases the local contrast, an important parameter of human visual perception [20], [21].

The main shortcomings of this technique and many other frequently applied image-restoration techniques are that only the magnitude of the frequency domain is manipulated, and the phase, which contains important information, is left unchanged. If an imaging model that describes phase changes occurring in cataract imaging can be developed, a far superior restoration could be obtained. It is also important to note that most of the techniques used are based on the least mean-square error criteria, which may not be appropriate for modeling of the best perceived image.

Acknowledgment

The authors thank S. Shapiro for valuable programming help and T. McInnes for technical help. The imaging work was performed at the Image Analysis Laboratory, New England Medical Center, Boston, MA.

References

[1] K. Leutwein and H. Littman, "The fundus camera," in *Refraction and Clinical Optics*, A. Safir, Ed. New York: Harper & Row, 1980, pp. 457-466.
[2] R. H. Webb, G. W. Hughes, and F. C. Delori, "Confocal scanning laser ophthalmoscope," *Appl. Opt.*, vol. 26, pp. 1492-1499, 1987.
[3] R. M. Davis, W. E. Humphrey, A. R. Kirschbaum, A. L. Shinn, and F. R. Stahr, "A new system for automated digital imaging and quantitative analysis of fundus images," in *Acta, XXV Concilium Ophthalmologicum*, Rome, Italy, 1986, F. C. Blodi, Ed. Amsterdam/Milan: Kugler/Ghedini, 1988, pp. 583-590.
[4] D. Wong, "Quality of fundus photograph affected by state of ocular media," *Ophthalmol. Times*, p. 44, June 1984.
[5] E. Fariza, A. E. Jalkh, J. V. Thomas, T. O'Day, E. Peli, and J. Acosta, "Use of circularly polarized light in fundus and optic disc photography," *Arch. Ophthalmol.*, vol. 106, pp. 1001-1004, 1988.
[6] J. Gilchrist, "Computer processing of ocular photographs—A review," *Ophthalmic Physiol. Opt.*, vol. 7, pp. 379-386, 1987.
[7] E. Peli, T. R. Hedges, and B. Schwartz, "Computerized enhancement of retinal nerve fiber layer," *Acta Ophthalmol.*, vol. 64, pp. 113-122, 1986.
[8] E. Peli and B. Schwartz, "Enhancement of fundus photographs taken through cataracts," *Ophthalmol.*, vol. 94(S), pp. 10-13, 1987.
[9] O. R. Mitchell, E. J. Delp, III, and P. L. Chen, "Filtering to remove cloud cover in satellite imaging," *IEEE Trans. Geosci. Electron.*, vol. GE-15, pp. 137-141, 1977.
[10] T. Peli and T. F. Quatieri, "Homomorphic restoration of images degraded by light cloud cover," in *Proc. ICASSP'84, IEEE Int. Conf. Acoust., Speech, Signal Processing*, 1984 (84 CH 1945), vol. 3, pp. 37.8.1-37.8.4.
[11] D. Miller and G. Benedek, *Intraocular Light Scattering*. Springfield, IL: Thomas, 1973, pp. 61-64.
[12] A. V. Oppenheim, R. W. Schafer, and T. G. Stockham, "Nonlinear filtering of multiplied and convolved signals," *Proc. IEEE*, vol. 56, pp. 1264-1291, 1968.
[13] T. Peli and J. S. Lim, "Adaptive filtering for image enhancement," *Opt. Eng.*, vol. 21, pp. 108-112, 1982.
[14] W. K. Pratt, *Digital Image Processing*. New York: Wiley, 1978, pp. 378-425.
[15] A. V. Oppenheim and R. W. Schafer, *Digital Signal Processing*. Englewood Cliffs, NJ: Prentice-Hall, 1975, pp. 532-571.
[16] G. Feigen, "Digital restoration of defocused images" (in Hebrew), Ph.D. dissertation, Dep. Appl. Phys., Hebrew Univ. Jerusalem, 1985.
[17] E. R. Cole, "The removal of unknown image blurs by homomorphic filtering," Ph.D. dissertation, Dep. Elec. Eng., Univ. Utah, Salt Lake City, ARPA Tech. Rep. UTEC-CSC-74-091, 1974.
[18] D. G. Falconer, "Image enhancement and film grain noise," *Opt. Acta*, vol. 17, pp. 643-705, 1970.
[19] V. T. Tom and G. J. Wolfe, "Adaptive histogram equalization and its applications," *Proc. SPIE (Appl. Digital Image Processing IV)*, vol. 359, pp. 204-209, 1982.
[20] E. Peli, "Perception of high-pass filtered images," *Proc. SPIE (Visual Commun. Image Processing II)*, vol. 845, pp. 140-146, 1987.
[21] D. A. Pollen, J. P. Gaska, and L. D. Jacobson, "Responses of simple and complex cells to compound sine-wave gratings," *Vision Res.*, vol. 28, pp. 25-39, 1988.